Single-shot three-dimensional shape measurement method using a digital micromirror device camera by fringe projection

著者	Ri Shien, Fujigaki Motoharu, Morimoto Yoshiharu
journal or publication title	Optical Engineering
volume	48
number	10
page range	103605
year	2009
URL	http://hdl.handle.net/10097/51970

doi: 10.1117/1.3250197

Optical Engineering 48(10), 103605 (October 2009)

Single-shot three-dimensional shape measurement method using a digital micromirror device camera by fringe projection

Shien Ri, MEMBER SPIE
Tohoku University
Graduate School of Engineering
Department of Nanomechanics
Aoba 6-6-01, Aramaki, Aoba-ku
Sendai 980-8579
Japan
E-mail: rishien@ism.mech.tohoku.ac.jp

Motoharu Fujigaki, MEMBER SPIE
Wakayama University
Faculty of Systems Engineering
Department of Opto-Mechatronics
930 Sakaedani
Wakayama 640-8510
Japan

Yoshiharu Morimoto, MEMBER SPIE
Moiré Institute
2–1–4–804, Hagurazaki, Izumisano
Osaka 598-0046
Japan

Abstract. We present a new single-shot 3-D shape measurement method using a digital micromirror device (DMD) camera and fringe projection. In optics of the DMD camera, individual DMD mirrors operate as controllable high-speed shutters for corresponding charge-coupled device (CCD) pixels. Therefore, four phase-shifted images can be recorded within one frame of the CCD camera by integrated phase-shifting methods using correlations. To obtain 3-D information of the object, an easy and accurate phase-to-3-D calibration method is performed. The principle and hardware are presented. The experimental results under dynamic conditions show that 3-D shape information can be analyzed from only a single image. © *2009 Society of Photo-Optical Instrumentation Engineers.* [DOI: 10.1117/1.3250197]

Subject terms: three-dimensional shape measurement; fringe projection; digital micromirror device camera; phase-shifting method; correlations; phase-to-3-D calibration method.

Paper 090452R received Jun. 19, 2009; revised manuscript received Aug. 23, 2009; accepted for publication Sep. 1, 2009; published online Oct. 26, 2009.

1 Introduction

Noncontacting shape measurement for 3-D objects is important in automated manufacturing, component quality control, reverse engineering, and so on.[1] Fringe projection profilometry combined with phase-shifting methods is a useful noncontact 3-D shape measurement technique. The phase-shifting method effectively attains high resolution and high accuracy in analyzing the phase of a projected grating.[2–4] This technique, however, is difficult to apply to dynamic conditions, since usually it requires several images.

To solve this problem, Huang and Chiang's group proposed a color-encoded digital fringe projection technique using a color camera and a digital micromirror device (DMD) projector.[5,6] Only one image of the object is required to obtain the 3-D surface contour of the object. In this technique, however, color separation and color balance compensation of RGB (color-coupling problem) are needed to obtain good measurement results. This means measurement errors could be introduced by the original color of the object surface.

Recently, we have developed a novel DMD camera[7,8] for phase analysis and shape measurement. In the DMD camera optics, individual DMD mirrors correspond to individual charge-coupled device (CCD) pixels. The direction of mirrors is controlled by digital signals in 30 μs or 1/1000 of the frame time of a conventional CCD camera, so the directions of DMD pixels are easily changed as needed while the CCD is capturing an image. In other words, individual DMD mirrors operate as controllable high-speed shutters for corresponding CCD pixels, and each pixel takes the integral value of the intensity while the shutter is open.

In this work, we propose a single-shot 3-D shape measurement using the DMD camera. Four phase-shifted images can be recorded within one frame of the CCD camera. To obtain the 3-D information of a shape, we use an accurate and easy phase-to-3-D calibration method, in which an LCD reference plane is used to calibrate the relationship between the phase value and the actual 3-D coordinates. Once the calibration procedure is completed, 3-D shape information can be analyzed from a single image.

This work is organized as follows. First, an outline of the DMD camera is introduced in Sec. 2. Then the principle of the single-shot shape measurement method is explained in Sec. 3. Section 4 shows experimental results both under static and dynamic conditions and a discussion is presented. Finally, Sec. 5 concludes the work.

2 Outline of the Digital Micromirror Device Camera

2.1 *What Is a Digital Micromirror Device Camera?*

A DMD[9–11] is an array of microscopic mirrors built over complementary metal oxide semiconductor static random access memory (CMOS SRAM) cells fabricated by semi-

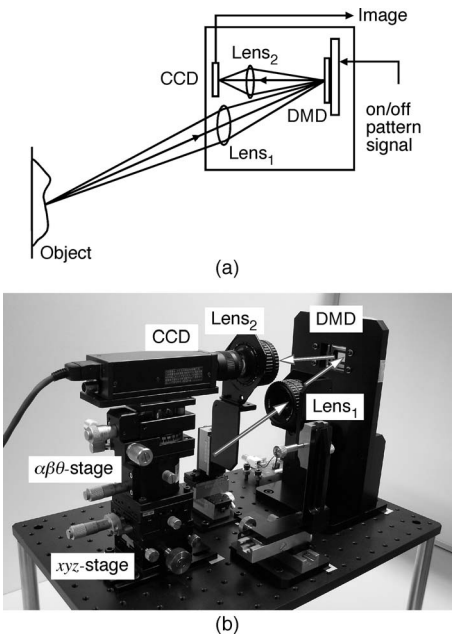

Fig. 1 DMD camera: (a) schematic structure and (b) photograph.

conductor manufacturing. Each mirror (13.7×13.7 μm) represents one pixel within the displayed image, and all mirrors on the array are independently modulated from on to off by applying an address voltage. Incident light is reflected in two directions according to the position of the DMD mirror, which depends on the on-off pattern signal transferred to the DMD by a computer. The mirror angle is −12 or +12 deg according to the on-off signal. For an incident angle of 24 deg, reflection angles are 0 deg if signals are on, and −48 deg if signals are off. The direction of each mirror is switched within 30 μs.

Recently, we have developed a new type of camera using a DMD device, i.e., the DMD camera, for phase analysis and shape measurement [see Fig. 1(a)]. The DMD camera consists of a DMD, a CCD, and two lenses (lens_1 and lens_2). An object is imaged on the surface of the DMD by lens_1. Each DMD mirror is imaged on the corresponding CCD pixel by lens_2. The DMD is used as a reflective spatial light modulator (SLM). If the DMD mirror is turned on, the light from a corresponding point on the object is reflected toward lens_2 and a light is imaged at the corresponding CCD pixel. If the DMD mirror is turned off, the light is not imaged on the corresponding CCD pixel. That is, each DMD mirror operates as a controllable high-speed shutter for the corresponding CCD pixel. Figure 1(b) shows the photograph of the DMD camera in our experiment. A CCD camera (Sony, XCD-X700; pixel size is 6.25×6.25 μm) is placed on an adjustable xyz stage and an $\alpha\beta\theta$-stage, which are movable and can tilt in three coordinates. The DMD accessory light modulator package (ALP) mentioned later and two Nikon EL-lenses ($f=50$ mm) are used.

2.2 *Features of the Digital Micromirror Device Camera*

Figure 2 shows the illustration of the relationship between a DMD on-off pattern and the captured image by the DMD camera. Figure 2(a) represents the image when all the mirrors of the DMD are set at the on position. When some DMD mirrors are set at the on position, as shown in Fig. 2(b), only the mirrors with on are imaged, as shown in Fig. 2(c). The on-off directions of each DMD mirror can be controlled by digital signals with 30 μs, which is approximately 1/1000 of the frame time of an ordinary CCD camera. For this reason, the directions of each DMD mirror can be easily changed multiple times while the CCD is capturing a single image. Each pixel of the CCD takes the integral value of the intensity while the shutter is opened. In this way, the advantage of the DMD camera is that each pixel of the CCD camera has a high-speed controllable shutter based on DMD technology.

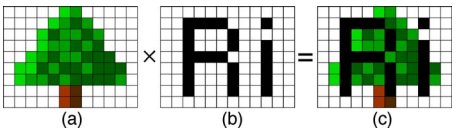

Fig. 2 Relationship between DMD on-off pattern and captured image by the DMD camera: (a) original image, (b) DMD on-off pattern, and (c) captured image by the DMD camera.

2.3 *Pixel-to-Pixel Correspondence*

In optics of the DMD camera, highly accurate pixel-to-pixel correspondence between the CCD and the DMD is important. We have proposed two pixel-to-pixel correspondence adjustment methods[12,13] using the moiré pattern caused by the difference in line spacing frequencies of the CCD and DMD. We display calibration patterns, which are 2-D periodic binary line gratings with 2- or 4-pixel spacing, on the DMD, and the image is captured by the CCD camera. If the CCD plane and the DMD plane are not parallel or image sizes on the CCD differ, i.e., when each mirror of the DMD and each pixel of the CCD do not correspond exactly, a moiré pattern appears after image processing. The moiré pattern is according to the position of the CCD camera, so we can determine mismatch and misalignment amounts from the moiré pattern and its phase distribution. As mismatch increases, the number of fringes in the moiré pattern increases, so we adjust xyz and $\alpha\beta\theta$ stages to decrease the moiré fringe until none appear in the image.[12] Furthermore, by analyzing phase distribution of the moiré fringe, adjustment error can be reduced to less than 1/25 of a pixel of the CCD.[13]

2.4 *High-Speed Control of Digital Micromirror Device Mirrors Using an Accessory Light Modulator Package Board*

Texas Instruments (TI, Dallas, Texas) introduced a Discovery 1100 general-purpose board to support new business areas as well as mainstream DMD technology in digital projection. Based on this Discovery 1100 platform, a German company, ViALUX (Chemnitz, Germany) developed an accessory light modulator package (ALP) parallel interface controller for high-speed DMD operation.[14,15] The key part of the ALP board is a Virtex-2 field programmable gate array (FPGA) linking on-board synchronous dynamic RAM (SDRAM) image memory with DMD data lines. The user PC interface is connected via a USB1.1 controller. The

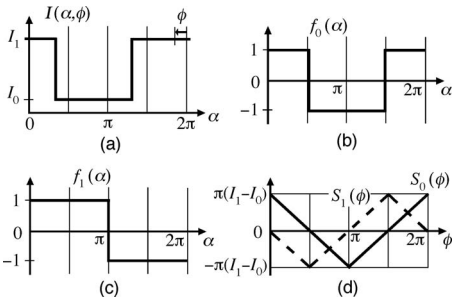

Fig. 3 Principle of the integrated phase-shifting method using correlations: (a) brightness distribution of a projected grating, (b) weight function of $f_0(\alpha)$, (c) weight function of $f_1(\alpha)$, and (d) integration values of $S_0(\phi)$ and $S_1(\phi)$.

ALP supports both binary and grayscale pattern sequences transferred to the DMD. A significant property is the perfect linearity of the time average output recorded by a synchronized camera. We use this DMD ALP for our experiment to control individual DMD mirrors at high speed. The minimum and maximum sequence display on times are 20 μm and 10 s. Frame rate is 6918 frames/s for binary image patterns. We make a synchronous controller to synchronize the DMD with other devices, i.e., the CCD camera and grating phase shifting.

3 Single-Shot Three-Dimensional Shape Measurement Method

3.1 *Principle of the Integrated Phase-Shifting Method Using Correlations*

A Ronchi grating is used in this method.[16] Figure 3(a) shows the brightness change of a projected rectangular grating at a point during phase shifting for one cycle with the initial phase ϕ. A Ronchi function $R(x)$ is defined as

$$R(x)=\begin{cases}1 & [\cos(x)\geqslant 0]\\ -1 & [\cos(x)<0]\end{cases}. \tag{1}$$

Intensity I at a point with the initial phase ϕ and the shifted phase α is represented as

$$I(\alpha,\phi)=\frac{I_1-I_0}{2}\cdot R(\alpha+\phi)+\frac{I_1+I_0}{2}, \tag{2}$$

where I_0 and I_1 are the higher and lower intensities, respectively, on the rectangular grating, as shown in Fig. 3(a). Two weight functions f_0 and f_1, as shown in Figs. 3(b) and 3(c), for the shifted phase α are defined as Eqs. (3) and (4), respectively.

$$f_0(\alpha)=\begin{cases}+1 & [\cos(\alpha)\geqslant 0]\\ -1 & [\cos(\alpha)<0]\end{cases}, \tag{3}$$

$$f_1(\alpha)=\begin{cases}+1 & [\sin(\alpha)\geqslant 0]\\ -1 & [\sin(\alpha)<0]\end{cases}. \tag{4}$$

Correlation functions S_0 and S_1, as shown in Fig. 3(d), are calculated as the integrations shown in Eqs. (5) and (6), respectively.

$$S_0(\phi)=\int_0^{2\pi} I(\alpha,\phi)\cdot f_0(\alpha)\mathrm{d}\alpha=\int_0^{\pi/2} I(\alpha,\phi)\mathrm{d}\alpha-\int_{\pi/2}^{3\pi/2} I(\alpha,\phi)\mathrm{d}\alpha+\int_{3\pi/2}^{2\pi} I(\alpha,\phi)\mathrm{d}\alpha, \tag{5}$$

$$S_1(\phi)=\int_0^{2\pi} I(\alpha,\phi)\cdot f_1(\alpha)\mathrm{d}\alpha=\int_0^{\pi} I(\alpha,\phi)\mathrm{d}\alpha-\int_{\pi}^{2\pi} I(\alpha,\phi)\mathrm{d}\alpha. \tag{6}$$

The initial phase ϕ can be obtained from correlation functions S_0 and S_1 as follows:

$$\phi=\left\{2+\frac{S_1}{|S_1|}+\frac{S_1\cdot S_0}{|S_1|\cdot(|S_0|+|S_1|)}\right\}\cdot\frac{\pi}{2}(0\leqslant\phi<2\pi). \tag{7}$$

3.2 *Single-Shot Phase Analysis Using the Digital Micromirror Device Camera*

Four images are recorded by the DMD camera during one cycle of phase shifting. Integrated values I_A, I_B, I_C, and I_D are the output brightness values of the DMD camera, and they are defined as integration of the intensity of the projected grating during phase shifting from 0 to $\pi/2$, from $\pi/2$ to π, from π to $3\pi/2$, and from $3\pi/2$ to 2π, respectively, as shown in Eq. (8).

$$\begin{cases} I_A=\int_0^{\pi/2} I(\alpha,\phi)\mathrm{d}\alpha\\ I_B=\int_{\pi/2}^{\pi} I(\alpha,\phi)\mathrm{d}\alpha\\ I_C=\int_{\pi}^{3\pi/2} I(\alpha,\phi)\mathrm{d}\alpha\\ I_D=\int_{3\pi/2}^{2\pi} I(\alpha,\phi)\mathrm{d}\alpha\end{cases}. \tag{8}$$

Equations (5) and (6) can be rewritten as Eq. (9) using the integral values I_A, I_B, I_C, and I_D.

$$\begin{cases} S_0=I_A-I_B-I_C+I_D\\ S_1=I_A+I_B-I_C-I_D\end{cases}. \tag{9}$$

The initial phase ϕ can be obtained from the brightness values I_A, I_B, I_C, and I_D by Eqs. (7) and (9).

Figure 4 shows a synchronization of the projected grating patterns of continuous phase shifting using a stepping motor and the DMD on-off patterns. DMD pattern pixels are grouped into A, B, C, and D. A DMD camera has controllable high-speed shutters for each pixel, as mentioned before. Patterns are changed regularly with $\pi/2$ phase shifting. CCD pixels of the groups A, B, C, and D are exposed by the DMD on-off patterns with phase shifting from 0 to $\pi/2$, $\pi/2$ to π, π to $3\pi/2$, and $3\pi/2$ to 2π, respectively. The integral values of the projected grating are recorded on each CCD pixel as integration while $\pi/2$ phase

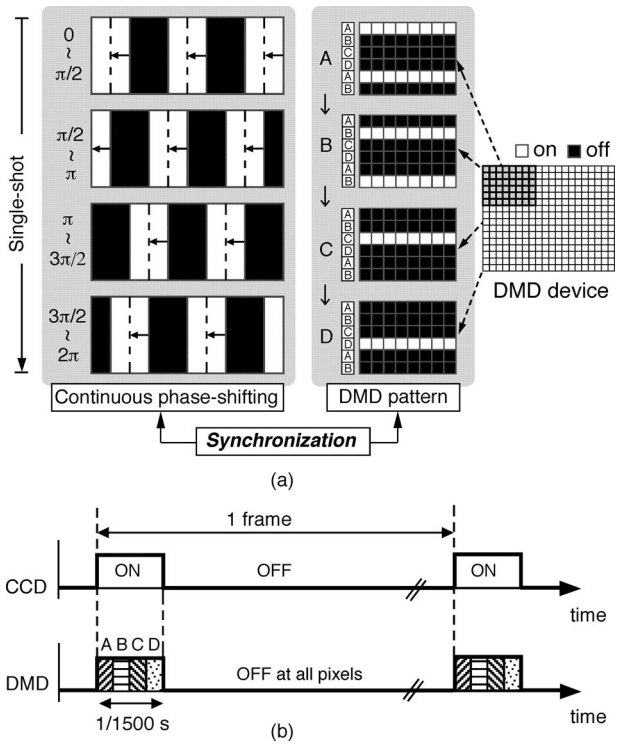

Fig. 4 Projected gratings and on-off patterns transferred to DMD to obtain phase distribution by the integrated phase-shifting method using correlations. (a) The synchronization of projected grating patterns and DMD on-off patterns. (b) The trigger timing between the CCD and DMD.

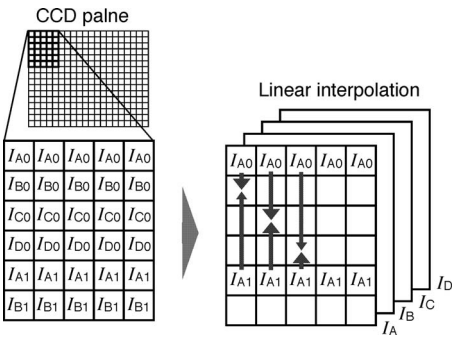

Fig. 5 Schematic explanation of interpolation to obtain four phase-shifted images.

shifting is being performed for each group. Integral values I_A, I_B, I_C, and I_D at a point are obtained by averaging with neighboring vertical pixels, as shown in Fig. 5. For example, the data I_B, I_C, and I_D at I_A are linearly interpolated by Eq. (10). So we obtain four phase-shifted images from a single image recorded using the DMD camera.

$$I_{A(i,j)} = I_{A(i,j)},$$

$$I_{B(i,j)} = \{I_{B(i,j-3)} + 3I_{B(i,j+1)}\}/4,$$

$$I_{C(i,j)} = \{I_{C(i,j-2)} + I_{C(i,j)+2}\}/2,$$

$$I_{D(i,j)} = \{3I_{D(i,j-1)} + I_{D(i,j+3)}\}/4. \quad (10)$$

Figure 4(b) shows the trigger timing between the CCD and the DMD. The DMD on-off patterns can be changed more than 6000 times in one second, i.e., a single shot can be performed theoretically within 1/1500 s. Therefore, shape measurement in dynamic conditions can be realized using this method.

3.3 *Phase-to-Three-Dimensional Calibration Method*

In phase-to-coordinate conversion, there are two approaches in optical triangulation profilometry: explicit and implicit calibration. Explicit calibration[17,18] requires the known geometric parameters of the optical setup, such as the distance between the projector center and the camera center, the distance between the camera center and the reference plane, and the angle between the projector and the camera axes. After the intrinsic and extrinsic parameter matrix of the camera and the projector are calibrated, the 3-D shape can be obtained by triangluar or stereo. Since the camera and/or projector are often described by a pinhole model with a linear model[19] or nonlinear model,[20] lens distortions of both the camera and the projector will decrease measurement accuracy, especially in the x and y coordinates. For this reason, it is difficult and time consuming to measure all geometric parameters precisely.

On the other hand, the implicit technique[21–24] is that phase-to-height mapping in a small local area is a linear transformation, and the coefficients of the linear transformation are different in different local areas. The implicit calibration technique usually works with a precise translation stage, on which a calibrated object is mounted. To calibrate the lateral xy coordinates, fiducial marks have to generally be attached to the calibration object.

Here, we use an easy and accurate phase-to-3-D implicit calibration method, which obtains the accurate xyz coordinates in each position using a reference plane, which is a liquid crystal display (LCD) panel coated with a diffusing film. The advantage of our method is that both the xy and z coordinates can be determined with high accuracy. The pitch of the LCD panel is manufacturing regularity with high accuracy. The LCD reference plane plays two important roles. One is projecting sinusoidal grating patterns by the projector (the power of the LCD panel is off) for calibrating the z coordinate, and the other is displaying sinusoidal grating patterns onto itself (the light from the projector is blocked) for calibrating the x and y coordinates. We analyze the phase of displayed fringe by the phase-shifting method; subpixel accuracy of x and y coordinates can be calibrated easily. The phase-to-3-D conversion is performed pixel by pixel. In our method, we do not use any geometric parameters. The actual xyz coordinates at each pixel are calibrated from the LCD reference at different positions. This means our method does not influence the lens distortions of a camera and/or a projector.

Figure 6 shows the optical geometry of our measurement system. First, reference phase ϕ_0, which represents the phase distribution of the reference plane at position z_0, is stored in a computer as the system characteristics. Then, the reference plane is moved to position z_1 by using an accurate linear stage, and the phase distribution ϕ_1 is ob-

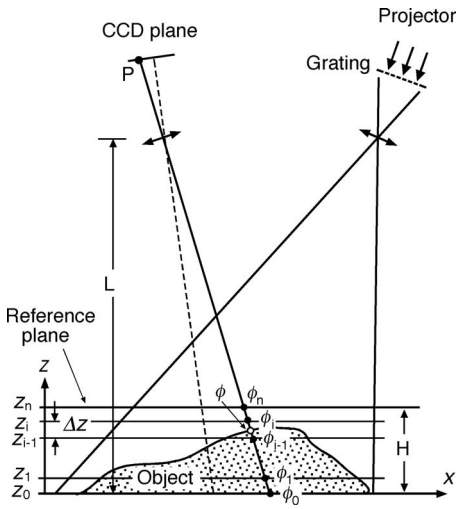

Fig. 6 Optical geometry of measurement system.

tained. By repeating this calibration procedure n times, the relationship between the phase values $\phi_0, \phi_1, \phi_2, \ldots, \phi_n$ and the height values $z_0, z_1, z_2, \ldots, z_n$ at each pixel can be obtained.

Figure 7 shows the case of point P in the CCD plane. The distance between the reference plane and the camera (L in Fig. 6) is larger than the interval of the two small reference planes. The phase value at each pixel in the CCD plane can be regarded as linear between z_i and z_{i-1}. In particular, we use multiple reference planes, and the interval of each two neighboring reference planes is much smaller than the distance L. The phase distribution caused by the distortion of the object is obtained as ϕ, and the height value can be calculated from two nearest reference planes z_i and z_{i-1} by linear interpolation in Eqs. (11) and (12):

$$(z_i - z_{i-1}):(z - z_{i-1}) = (\phi_i - \phi_{i-1}):(\phi - \phi_{i-1}), \tag{11}$$

$$z = \frac{(z_i - z_{i-1})(\phi - \phi_{i-1})}{(\phi_i - \phi_{i-1})} + z_{i-1}. \tag{12}$$

For example, the height of phase ϕ_P in Fig. 7 is calculated from ϕ_{i-1} and ϕ_i by linear interpolation. On the other hand, the height of phase ϕ_Q is calculated from ϕ_{k-1} and $\phi_k + 2\pi$, not ϕ_{k-1} and ϕ_k, because the phase value is in the phase jumping area.

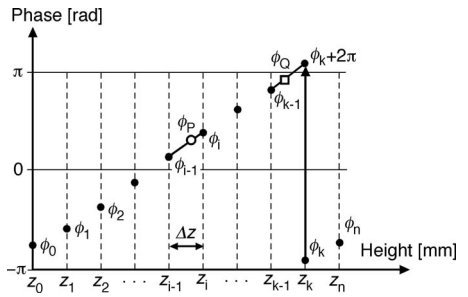

Fig. 7 Relationship between phase values and actual heights at points P and Q in the camera plane.

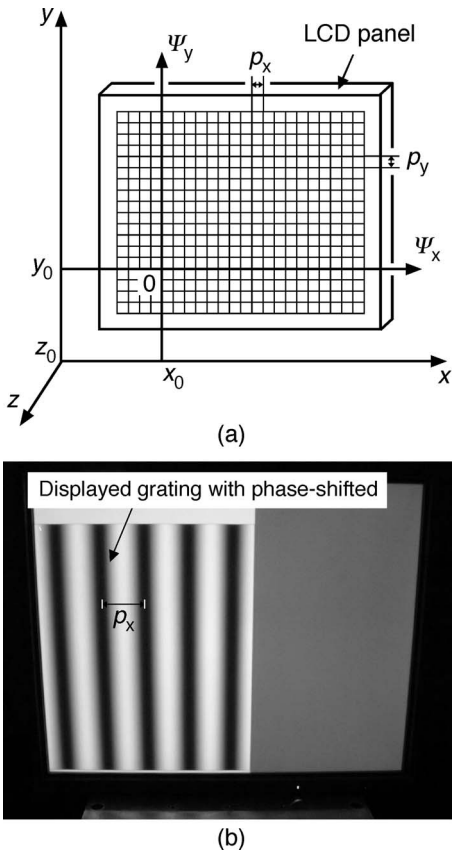

Fig. 8 LCD reference plane for calibrating *x*, *y*, and *z* coordinates of each position: (a) *xyz* coordinate; and (b) a photograph when the sinusoidal grating is displayed in the LCD reference plane for calibrating the *x* and *y* coordinates.

Secondly, we calibrate the lateral x and y coordinates by displaying sinusoidal 2-D grating patterns with multiple phase shifts on the reference plane (LCD panel). Figure 8 shows the LCD reference plane for calibrating x, y, and z coordinates of each position. Figure 8(a) is the global xyz coordinate and Fig. 8(b) shows a photograph when the sinusoidal grating is displaying onto itself for calibrating x and y coordinates. The grating pattern on the right side of Fig. 8(b) is not displayed intentionally to confirm how it works. In an experiment of 3-D measurement, a grating pattern is displayed in all areas. The sinusoidal grating is displayed separately in x and y directions instead of a 2-D grating.

In Fig. 8(a), the regular pitches of the grating are defined as p_x and p_y in the x and y directions, respectively. The 2-D phases are analyzed by the phase-shifting method. After the unwrapped 2-D phases (Ψ_x, Ψ_y) from positions z_0 to z_n are analyzed, the x and y coordinates on the reference plane at position z_i can be obtained from the 2-D phases (Ψ_{xi}, Ψ_{yi}) as follows:

$$x_i = \frac{p_x \psi_{xi}}{2\pi} + x_0,$$

$$y_i = \frac{p_y \psi_{yi}}{2\pi} + y_0, \tag{13}$$

where x_0 and y_0 are the coordinates of the point at which the 2-D phases (Ψ_{xi}, Ψ_{yi}) are equal to (0, 0). After the phase-to-height relationship is determined, the x and y coordinates can be converted by Eqs. (14) and (15):

$$(x_i - x_{i-1}):(x - x_{i-1}) = (z_i - z_{i-1}):(z - z_{i-1}),$$

$$(y_i - y_{i-1}):(y - y_{i-1}) = (z_i - z_{i-1}):(z - z_{i-1}), \tag{14}$$

$$x = \frac{(x_i - x_{i-1})(z - z_{i-1})}{(z_i - z_{i-1})} + x_{i-1},$$

$$y = \frac{(y_i - y_{i-1})(z - z_{i-1})}{(z_i - z_{i-1})} + y_{i-1}. \tag{15}$$

The 3-D coordinates at each pixel can be calculated in the same manner.

4 Experiment

4.1 *System Setup*

A personal computer (CPU Intel Core2, 2.4 GHz, memory 2-GB RAM) digitizes the image, produces the DMD on-off patterns, and transfers it to the DMD board in advance. The phase shifitng of a film grating is performed by a linear stepping motor mechanically. A synchronous controller synchronizes the phase shifting of a film grating, the DMD on-off patterns, and the CCD capture timing. The pitch $p_x(=p_y)$ of the displayed sinusoidal grating pattern at the LCD panel is 16 pixels, and it corresponds to 4.224 mm. 16-step phase-shifted patterns are displayed by shifting each one pixel both in x and y directions.

In this experiment, a soft balloon is measured at a frame rate of the CCD (15 frames/s). The CCD's shutter speed is 66.7 ms, and the exposure time of each DMD on-off pattern (A, B, C, and D) is 16.6 ms. Six reference planes at 3.0-mm intervals are used. The distances to the object from the projector and the DMD camera are 560 and 1260 mm, respectively. The angle between the projector and the DMD camera is 24 deg.

4.2 *Experimental Results*

Figure 9 shows the 3-D measurement result of pushing a balloon under dynamic conditions. Figure 9(a) shows the single captured image (640 pixels × 480 pixels) using the DMD camera, and the small image window on the left side shows further details of the grating pattern. Figure 9(b) shows the four phase-shifted grating images (I_A, I_B, I_C, and I_D) produced from Fig. 9(a) by linear interpolation. Figure 9(c) shows the wrapped phase distribution ϕ by the integrated phase-shifting method using correlations. Figure 9(d) shows the distributions of the xyz-coordinate by the proposed calibration method, and the 3-D mesh representation of the central area of Fig. 9(d) is shown in Fig. 9(e). A 3-D shape of the object can be obtained from one image,

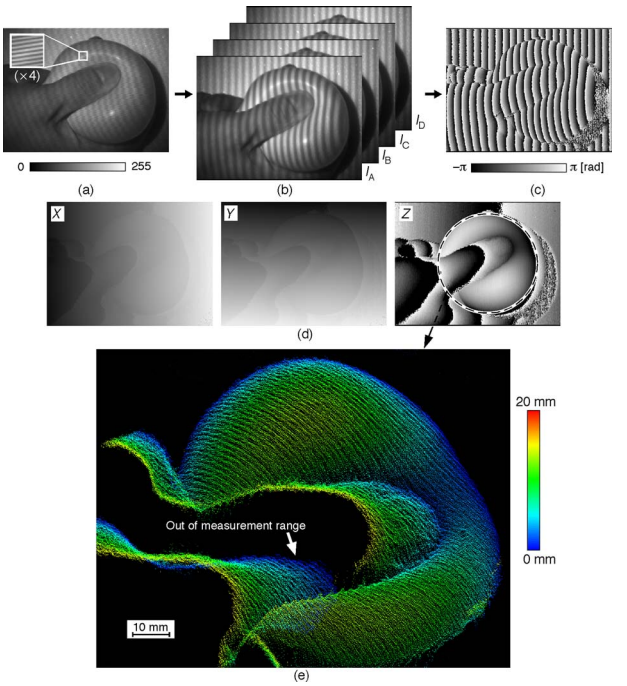

Fig. 9 3-D measurement result of pushing a balloon under dynamic conditions. (a) One-shot image captured by the DMD camera. The small image window on the left side shows further details. (b) The four phase-shifted grating image (I_A, I_B, I_C, and I_D) produced from (a) by linear interpolation. (c) Wrapped phase distribution ϕ obtained from (b). (d) Distributions of xyz coordinate. (e) 3-D mesh representation of the central area of (d).

i.e., Fig. 9(a). Figure 10 shows the experimental result of pushing a balloon under dynamic conditions from $t=0$ s to $t=56/15$ s.

To estimate the accuracy of the present method, a planar surface (the reference plane) is measured under static and dynamic conditions. Figure 11 shows the 3-D measurement result of the plane at position $z=9$ mm in static condition. The height distribution is shown in Fig. 11(a), and one cross section is shown in Fig. 11(b). The average error is 39 μm and the standard deviation is 79 μm. Under dynamic conditions, the flat plane moving normal to the z axis is measured. We measured ten different positions at a constant speed of 10 mm/s. The image capture interval is 0.142 s, and the theoretical distance of the flat plane between the adjacent frame is 1.42 mm. Figure 12 shows the measured distance of adjacent frames. The average error is 90 μm and the standard deviation is 160 μm.

4.3 *Discussions*

This method is applicable to dynamic phenomenon, because only a single image is needed to obtain the 3-D coordinates. Singe-shot 3-D measurement can be performed theoretically within 1/1500 s, because the DMD on-off pattern can be changed more than 6000 times in one second. In the present experiment, current performance (15 fps) is restricted by phase-shifting speed. High-speed phase shifting is now under study to improve the data acquisition speed, so that the errors caused by motion will be reduced.

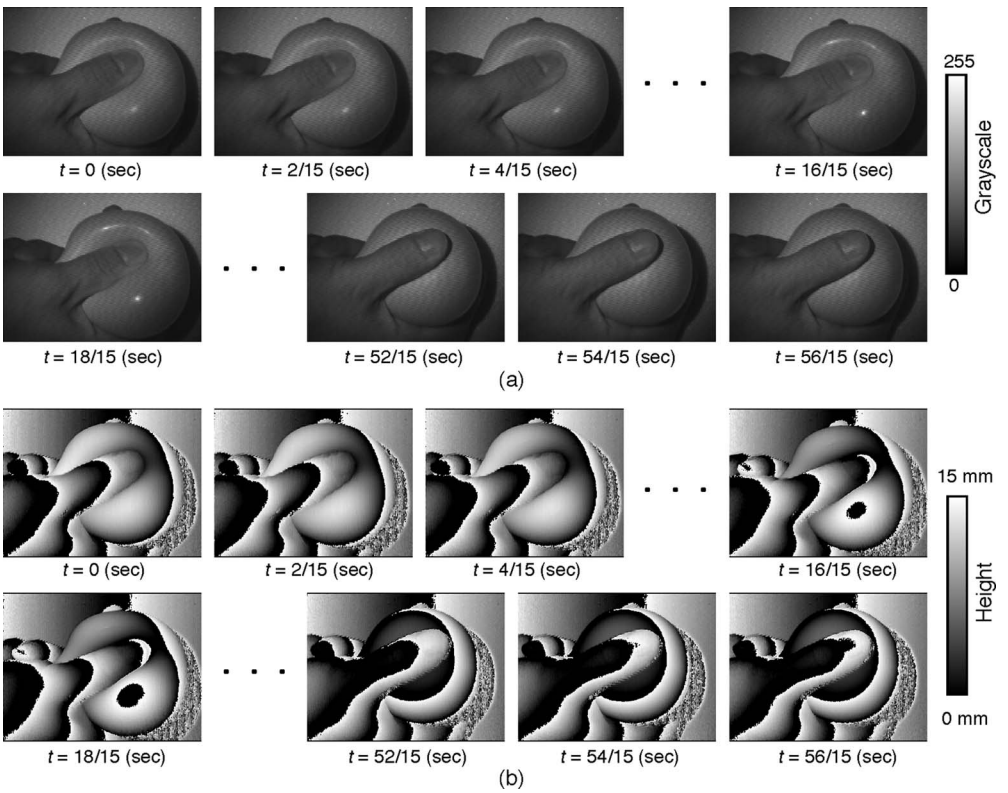

Fig. 10 Experimental results of pushing a balloon under dynamic conditions: (a) single-shot images and (b) height distributions.

A flat plane is also measured without interpolation to investigate how the image interpolation as mentioned in Sec. 3.2, affects the measurement quality. Comparing the phase distributions with and without interpolation, the average error is 0.013 radians (0.2% with 2π range), and the standard deviation is 0.0816 radians (1.3% with 2π range). The error due to interpolation is less than 1.5%. However, it is difficult to measure objects with high slope and discontinuities. In this case, a camera and a DMD with high resolution are preferred for measurement.

The current system is good enough to measure dynamic shapes within a small depth range. However, the measurement range is limited to about 15 mm because we do not perform phase unwrapping along the z coordinate. In Fig. 9, therefore, the fingertips and the top of the balloon are in the correct measurement range. On the other hand, the hand and background are out of the measurement range. The expansion of dynamic range is our future work.

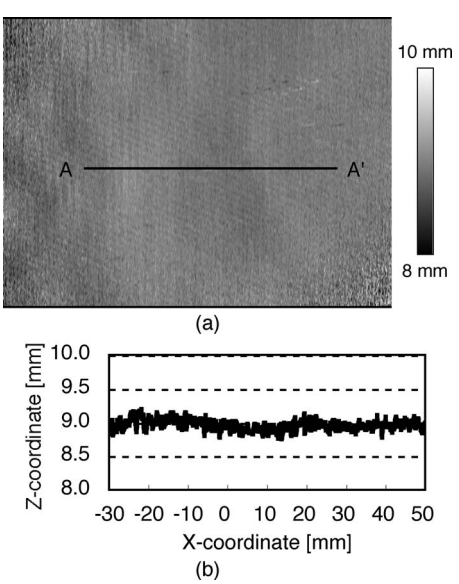

Fig. 11 3-D measurement result of a planar surface (the reference plane at position z=9 mm) at static condition: (a) height distribution and (b) cross section along line AA′. The average error is 39 μm and standard deviation is 79 μm.

5 Conclusions

We present a single-shot shape measurement method using the DMD camera. Four phase-shifted images can be re-

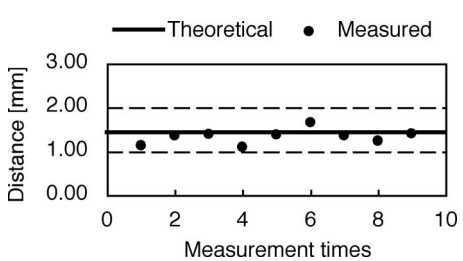

Fig. 12 Measured distance of adjacent frames at a constant 10 mm/s. The average error is 90 μm and the standard deviation is 160 μm.

corded within one frame of the CCD camera by an integrated phase-shifting method using correlations. To determine the 3-D information of the object, an accurate and easy coordinate calibration method by using an LCD reference plane is performed. The experimental results under dynamic conditions show that 3-D shape information can be analyzed from only a single captured image. Performing high-speed phase shifting to improve the data acquisition speed and expansion of the dynamic range is our future work. Such a system will be useful for mechanical engineering, sport engineering, medical imaging, etc.

References

1. F. Chen, G. M. Brown, and M. Song, "Overview of three-dimensional shape measurement using optical methods," *Opt. Eng.* **39**(1), 10–22 (2000).
2. V. Srinivasan, C. Liu, and M. Halioua, "Automated phase-measuring profilometry of 3-D diffuse objects," *Appl. Opt.* **23**(18), 3105–3108 (1984).
3. H. O. Saldner and J. M. Huntley, "Profilometry using temporal phase unwrapping and a spatial light modulator based fringe projector," *Opt. Eng.* **36**(2), 610–615 (1997).
4. S. Kakunai, T. Sakamoto, and K. Iwata, "Profile measurement taken with liquid-crystal gratings," *Appl. Opt.* **38**(13), 2824–2828 (1999).
5. P. S. Huang, Q. Hu, F. Jin, and F. P. Chiang, "Color-encoded digital fringe projection technique for high-speed three-dimensional surface contouring," *Opt. Eng.* **38**(6), 1065–1071 (1999).
6. J. Pan, P. S. Huang, and F. P. Chiang, "Color phase-shifting technique for three-dimensional shape measurement," *Opt. Eng.* **45**(1), 013602 (2006).
7. M. Fujigaki, Y. Morimoto, and Q. Gao, "Shape and displacement measurement by phase-shifting scanning moiré method using digital micro-mirror device," *Proc. SPIE* **4537**, 362–365 (2002).
8. S. Ri, M. Fujigaki, and Y. Morimoto, "Intensity range extension method for three-dimensional shape measurement in phase-measuring profilometry using a digital micromirror device camera," *Appl. Opt.* **47**(29), 5400–5407 (2008).
9. L. J. Hornbeck, "Deformable-mirror spatial light modulators," *SPIE Crit. Rev. Series* **1150**, 86–102 (1989).
10. J. B. Sampsell, "An overview of the digital micromirror device (DMD) and its application to projection displays," *SID Int. Symp. Digest Tech. Papers*, **24**, 1012–1015 (1993).
11. L. J. Hornbeck, "Digital light processing for high-brightness, high-resolution applications," *Proc. SPIE* **3013**, 27–40 (1997).
12. S. Ri, M. Fujigaki, T. Matui, and Y. Morimoto, "Pixel-to-pixel correspondence adjustment in DMD camera by moiré methodology," *Exp. Mech.* **46**, 67–75 (2006).
13. S. Ri, M. Fujigaki, T. Matui, and Y. Morimoto, "Accurate pixel-to-pixel correspondence adjustment in a digital micromirror device camera by using the phase-shifting moiré method," *Appl. Opt.* **45**(27), 6940–6946 (2006).
14. W. Osten, T. Haist, and K. Korner, "Active approaches in optical metrology," *Proc. Intl. Conf. Laser Appl. Opt. Metrol.*, pp. 9–19 (2003).
15. R. Hofling and E. Ahl, "ALP: universal DMD controller for metrology and testing," *Proc. SPIE* **5289**, 322–329 (2004).
16. Y. Morimoto, M. Fujigaki, and H. Toda, "Real-time shape measurement by integrated phase-shifting method," *Proc. SPIE* **3744**, 118–125 (1999).
17. Q. Hu, P. S. Huang, Q. Fu, and F. P. Chiang, "Calibration of a three-dimensional shape measurement system," *Opt. Eng.* **42**(2), 487–493 (2003).
18. S. Zhang and P. S. Huang, "Novel method for structured light system calibration," *Opt. Eng.* **45**(8), 083601 (2006).
19. Z. Zhang, "A flexible new technique for camera calibration," *IEEE Trans. Pattern Anal. Mach. Intell.* **22**(11), 1330–1334 (2000).
20. J. Weng, P. Cohen, and M. Herniou, "Camera calibration with distortion models and accuracy evaluation," *IEEE Trans. Pattern Anal. Mach. Intell.* **14**(10), 965–980 (1992).
21. W. S. Zhou and X. Y. Su, "A direct mapping algorithm for phase-measuring profilometry," *J. Mod. Opt.* **41**(1), 89–94 (1994).
22. G. Sansoni, M. Carocci, and R. Rodella, "Calibration and performance evaluation of a 3-D imaging sensor based on the projection of structured light," *IEEE Trans. Instrum. Meas.* **49**(3), 628–636 (2000).
23. B. A. Rajoub, D. R. Burton, and M. J. Lalor, "A new phase-to-height model for measuring object shape using collimated projections of structured light," *J. Opt. A, Pure Appl. Opt.* **7**, s368–s375 (2005).
24. Z. H. Zhang, D. P. Zhang, X. Peng, and X. T. Hu, "Performance analysis of a 3D full-field sensor based on fringe projection," *Opt. Lasers Eng.* **42**, 341–353 (2004).

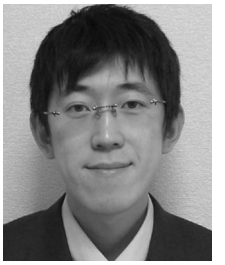

Shien Ri received his master's and PhD degrees in systems engineering from Wakayama University in 2004 and 2007, respectively. He received the Fellowship of the Japan Society for the Promotion of Science for Young Scientists from 2006 to 2008. Currently, he is an assistant professor at the Department of Nanomechanics, Tohoku University. He is a member of the OSA, SPIE, SEM, the Japan Society of Experimental Mechanics, the Japan Society of Mechanical Engineers, and the Japanese Society for Nondestructive Inspection. He received the Encouragement Award for Promising Researchers from the Japan Society of Experimental Mechanics in 2007. His major research interests are optical methods, 3-D shape measurement, advanced image processing, and experimental mechanics.

Motoharu Fujigaki received his BE and ME degrees in mechanical engineering from Osaka University in 1990 and 1992, respectively. He received his doctoral degree from Osaka University in 2001. He was working in NABCO Limited from 1992 to 1995. He moved to Wakayama University in 1995. Now he is an associate professor in the Department of Opto-Mechatronics, Faculty of Systems Engineering, Wakayama University. He is interested in optical metrology using image processing, especially shape and deformation measurement using gating projection methods, and small displacement measurement using laser interferometry. He is a member of SPIE, SEM, Japan Society of Experimental Mechanics, and Japan Society of Mechanical Engineers.

Yoshiharu Morimoto is the representative director of the Moiré Institute in Japan. He graduated from of Osaka University, Japan, in 1968. He is a JSME Fellow and Honorary Member of JSEM. He was a member of the SEM Executive Board, Chairman of ACEM, and President of JSEM. He was a researcher of Komatsu Manufacturing, Limited, associate professor of Osaka University, professor of the Department of Opto-Mechatronics of Wakayama University, and vice-president of Wakayama University. His major field of study is photomechanics, i.e., experimental mechanics using optics and image processing. His current interests are development of measurement methods and equipment for shape, deformation, stress, and strain using moiré methods and phase-shifting digital holographic interferometry.